Turk J Phys
() : –
© TÜBİTAK
doi:10.3906/fiz-

Assesement of Cyclotron Produced ^{64}Cu Radionuclide with Monte Carlo Simulations

Aydın Yıldırım[1,*], **İsmail Boztosun**[2]
[1]Proton Accelerator Facility, TENMAK-NÜKEN, Ankara, Türkiye
[2]Physics Department, Akdeniz University, Antalya, Türkiye

Received: .. 2023 • **Accepted/Published Online:** .. 20.. • **Final Version:** .. 20..

Abstract: Physical yields and activities of theranostic radioisotope ^{64}Cu were calculated via Monte Carlo simulations. Geant4 simulation toolkit is employed for the Monte Carlo calculations. The study is based on proton irradiation of solid targets at cyclotron facilities. Two types of target material were investigated: Nickel and Zinc. Also, two different target thickness and two beam angles were assessed in order to see the change of yields and activities. The optimum results were achieved at 150 μm thickness, 24 MeV beam energy and 5° beam angle for the nickel target, and 150 μm thickness, 30 MeV beam energy and 5° beam angle for the zinc target.

Keywords: Copper-64, Cyclotron, Monte-Carlo, Radioisotope, Radiopharmaceutical

1. Introduction

Nuclear medicine applications are becoming more and more extensive around the world, mainly because of the vast variety of cancer types. Furthermore, it is not limited to only cancer diagnosis and treatment. There are several nuclear medicine applications for other types of diseases like cardiovascular and neurological, which use nuclear medicine for diagnostic purposes [1]. The main component of nuclear medicine is radioisotopes. Radioisotopes play a critical role in nuclear medicine applications because they can be used for both diagnostic and therapeutic purposes. While traditional radioisotopes like ^{11}C, ^{15}O, ^{15}N, ^{18}F, ^{124}I have been in use for quite some time and are acknowledged in medical applications, there are newer types of radioisotopes that can also be used for diagnostic and therapeutics at the same time, and their applications are called "theranostic" [2–7]. With the development of the technology, nuclear medicine applications are also developed. Instead of using common diagnostic and treatment methods, medical centers started to use personalized medicines, which are more effective [2–4, 8]. But these kind of applications may be expensive than traditional methods. Furthermore, in order to use personalized nuclear medicines or more clearly radioisotopes, first one needs to produce the interested radioisotope with enough activity. And this may be even a bigger problem than the price of the medicine. Radioisotopes can be produced in research reactors or particle

*Correspondence: aydinyldrm@gmail.com

accelerators. Building a research reactor solely for radioisotope production is not only expensive, but also inefficient. Particle accelerators are well-suited for radioisotope production, and there are several accelerators around the world. However, many of these accelerators produce only traditional radioisotopes, and their beam time is often limited. As a result, these invaluable infrastructures are not being utilized with sufficient efficiency. The newer radioisotopes can be produced in particle accelerators with enough research and development and also dedicated time [9].

^{64}Cu is an emerging radioisotope in nuclear medicine which can be used for both diagnostic and therapeutics because of its unique physical properties [10–17]. The half-life of ^{64}Cu is $t_{1/2} = 12.7h$ and it has three different decay modes: β^+ (17.5 %), β^- (38.5 %) and, electron capture (EC 44 %) [4]. ^{64}Cu can be used for positron emission tomography (PET) imaging as an alternative to ^{18}F. Furthermore, its half-life is longer than that of ^{18}F and other traditional PET radioisotopes, so this radioisotope can be produced centrally and distributed without losing too much activity [6]. It is reported that the ^{64}Cu is very effective for the diagnosis of hypoxia tumor [14, 18]. Also, it is an advantageous radioisotope because it is easily soluble in water and has +2($CuCl_2$) oxidation state, which means it can be used to make many radiotracers [18, 19]. It is also reported that the ^{64}Cu has been successfully used for high-quality imaging of blood flow in the primate brain and dog kidney and heart [14]. The remaining decay modes of ^{64}Cu, which are β^- and EC, results with Auger electrons, and they are used for targeted radionuclide therapy [20, 21]. In addition, the radioisotope has a growing interest in macro-molecule labeling such as peptide, protein, monoclonal antibodies, etc. [16, 22].

Although ^{64}Cu is highly useful and of increasing importance, its production is not sufficient to meet the need. The most important reason is that the reaction most commonly used to produce ^{64}Cu requires enriched ^{64}Ni [4]. Since enriched ^{64}Ni is very expensive, accelerator facilities prefer to produce traditional radioisotopes over ^{64}Cu [1, 2, 11]. The aim of this study is to investigate the reaction channels for ^{64}Cu, which can be produced in accelerator facilities, and to obtain the optimum irradiation parameters when using enriched or unenriched targets. In the study, the reaction channels will be analyzed for different energies and currents in both target cases and the target activities and physical yields will be presented accordingly. This paper is organized as follows: in Section 2, possible reaction channels for ^{64}Cu production will be provided, and the Monte Carlo technique, which will be used in the study, will be introduced. In Section 3, each reaction channel will be investigated in the enriched and unenriched target cases, and the activities and physical yields obtained at the end of irradiation will be discussed. The Section 4 will conclude the study.

2. Methodology

2.1. Targetry

There are several reaction channels that can be used to produce the desired radioisotope ^{64}Cu, including the use of proton, deuteron or neutron beams on solid targets. As proton accelerators are more common, we investigated the proton-induced reaction channels. Two target materials, nickel and zinc, are potential candidates for the production of ^{64}Cu. Although enriched materials are usually preferred for the production of ^{64}Cu, we have studied both enriched and elemental materials in our research. The need for enriched targets may also be reduced in some cases by the study of new target systems and the use of high-current accelerators.

Considering both cases (enriched and elemental), four target possibilities were investigated: ^{nat}Ni, ^{64}Ni, ^{nat}Zn and ^{68}Zn. As the physical yield obtained varies with target thickness, all targets were irradiated in two different thicknesses for comparison. The first thickness was taken as 100 μm and the second as 150 μm. Another aspect of target irradiation is the angle the target makes with the horizontal plane. As often found in the literature, placing the target perpendicular to the horizontal plane will cause the target to overheat at high currents. If the target is not sufficiently cooled, it will be damaged. For this reason, solid target systems in accelerator facilities are designed at a slight angle to the beam direction. In such designs, the incoming beam spreads out over the target rather than hitting it directly. The tilt angle may depend on the cyclotron specifications or the solid target design, and varies between 5° and 26° in different studies [1, 23–25]. In any case, the power density incident on the target can be kept at a low level. Two different angles were chosen for the study, 5° and 10°. All targets and fixed target inclinations were studied with simulations. The main objective is to evaluate the possible routes to produce ^{64}Cu with sufficient activity, i.e. the target activity can be used for patient treatment. The routes investigated include enriched materials and as the enriched materials are very expensive, optimisation by simulation is essential for this type of work.

2.2. Monte Carlo Simulations

This study is based on Monte Carlo simulations and uses the Geant4 toolkit to calculate physical yields after irradiation. Geant4 is a powerful Monte Carlo simulation application with a large and up-to-date database of nuclear interactions [26–28]. The Geant4 graphical user interface (GUI), although a code-based simulation application, allows the user to check the design geometry, control the visualisation, use different beams and particles, and create any desired setup with great flexibility. It is also very flexible to create any geometry for the desired setup.

The Geant4 physics list "QGSP_BERT_HP" was used for the physical yield and activity calculations. The G4TENDL-1.4 dataset was also used for cross sections. Geant4 is normally used for high energy physics, so most of the physics lists are for higher energies. As we are interested in energies between 10 MeV and 30 MeV there are only a few options for the physics list and QGSP_BERT_HP is one of them [29]. The geometry was created using target material, copper backing and aluminium target holder. The beam has a diameter of 1 cm and a Gaussian profile. The components of the setup are shown in Figure (1). The simulation application provides a ROOT output by default. On completion of the simulation, the ROOT software was used to evaluate the results (see also "ROOT" [software], release v6.24/06, 03/09/2021, https://root.cern/releases/release-62406/). [30].

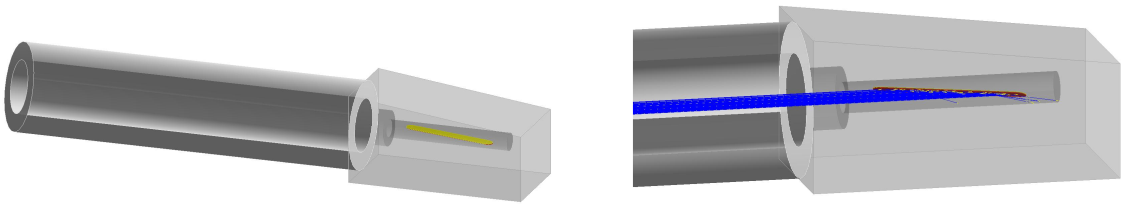

(a) (b)

Figure 1: Simulation setup of solid target. The simulation includes beam line (dark grey cylinder), Nickel or Zinc target (red), backing copper (yellow), Aluminum target holder (transparent grey trapezoid). Blue lines show the proton beam coming from the '-z' direction.

3. Results

We have studied the physical yields of the different targets under proton bombardment in order to assess the activity of ^{64}Cu at the end of bombardment (EOB). The study also includes the cooling time of the bombarded target to reach the required radionuclide purity, which is usually higher than 99% for the radioisotope of interest. The possible pathways and the effect of target thickness are discussed below.

3.1. Nickel Target

Nickel is the most commonly used target to produce the radioisotope ^{64}Cu using proton irradiation for medical applications. The reaction channel for this target is ^{64}Ni(p,n)^{64}Cu. We have investigated two possible cases for the nickel target. The first is elemental nickel and the second is enriched nickel. Although the same reaction channel is used for both targets, the ratio of ^{64}Ni in the target directly affects the activity at the EOB. The elemental nickel consists of 68.077% ^{58}Ni, 26.223% ^{60}Ni, 1.140% ^{61}Ni, 3.635% ^{62}Ni and 0.926% ^{64}Ni. in the Geant4 material database. However, the enriched nickel targets usually contains $> 99\%$ of ^{64}Ni. For the evaluation of the target irradiation we choose an energy interval between 10 MeV - 30 MeV. Both the physical yield and the activity of ^{64}Cu are given in tables in the appendix (see tables 1 and 2 in the Appendix section 5). For the activity calculations 200 μA current and 3 hours irradiation time were chosen. The physical yields after irradiation are also shown in Figure (2). There are 8 different results shown in Figure (2). The figure includes two different target thicknesses, two different irradiation tilt angles and also the two target types: elemental and enriched. The physical yield values on the vertical axis are given in logarithm. In the previous works of Szelecsenyi et al. [31], Avila-Rodriguez et al. [32], Aslam et al. [33] and Rebeles et al. [34] the 10 - 13 MeV range is measured with the highest cross section for the ^{64}Ni(p,n)^{64}Cu reaction channel.

In the present study we have calculated that the 13-25 MeV range has the highest yield for ^{64}Cu in this type of tilted target systems. We have also seen that the 5° inclination and 150 μA thick enriched target configuration maintains its high yield of ^{64}Cu up to 30 MeV, while the other enriched targets have relatively lower yields.

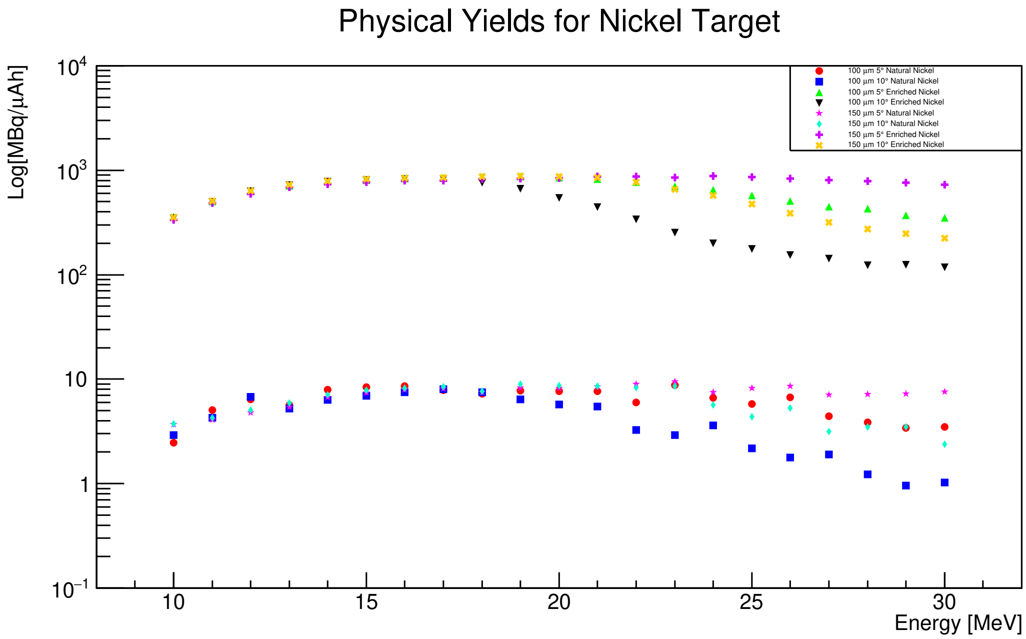

Figure 2: The physical yields of the Nickel target. All the configuration for Nickel target are presented in the figure. The vertical axis in logarithmic scale.

The target prepared from the natural nickel gives also a substantial yield of ^{64}Cu as presented in both Figure (2) and Tables (1) and (2). The energy range of 15 - 22 MeV seems to have the highest yield of ^{64}Cu. Although the physical yields of ^{64}Cu can go higher with increasing irradiation time, the natural target may not be the best option for producing ^{64}Cu. While the enriched targets which are used in medical applications are extremely expensive, they usually have more than one advantages. In the ^{64}Cu case, when irradiating the natural nickel targets, other copper isotopes are also produced along with ^{64}Cu. Although the half-lives of these isotopes relatively short and they decay much faster than ^{64}Cu, they still remain in the final product. The chemical processes cannot eliminate these side products and they end up with the patient dose. In order to reach the specific activity which required for the patient, the copper ratio should be increased in the radiopharmaceuticals. This may lead to a high dose of metal absorption of the body. Thus, the uses of enriched target material of nickel is the safest route for the patient's health.

3.2. Zinc Target

Another alternative target to ^{64}Cu production is zinc. We followed the same procedure to assess the yields for this target. Two different thicknesses, two different inclination angles were chosen for both natural and enriched zinc. The natural zinc consists of 48.630% ^{64}Zn, 27.900% ^{66}Zn, 4.100% ^{67}Zn, 18.750% ^{68}Zn and 0.620% ^{70}Zn in the Geant4 material database. This time ^{68}Zn was used for the enriched material and the expected reaction is $^{68}Zn(p,x)^{64}Cu$. The results are given in Figure (3), Table (3) and Table (4). It can be seen from Figure (3) that the yields increase with energy in all cases and the yields do not differ too much for the type of target (natural or enriched) as in the case of the nickel target. It seems that the 30 MeV beam energy gives the highest yield for all the setups studied. Furthermore, it seems that the angles and the thickness of the target do not cause a significant change in the yield. There is another notable feature for the enriched target. The production of ^{64}Cu does not start before 19 - 20 MeV. But the other reaction channels other than $^{68}Zn(p,x)^{64}Cu$ lead to the production of ^{64}Cu at lower energies in the natural zinc target.

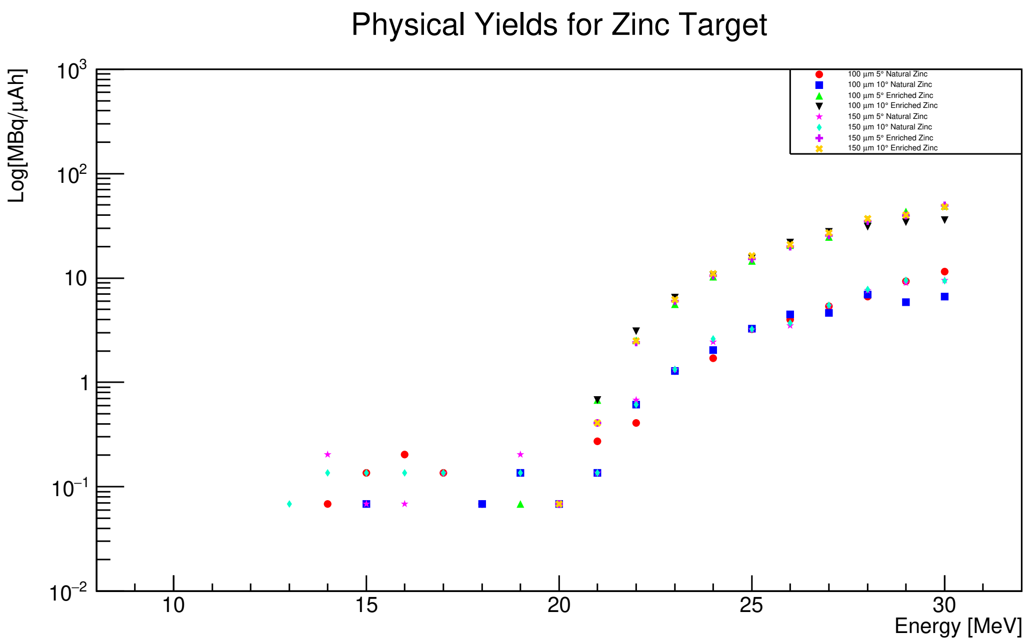

Figure 3: The physical yields of the Zinc target. All the configuration for Zinc target are presented in the figure. The vertical axis in logarithmic scale.

4. Conclusion

We have evaluated the two target alternatives for the production of ^{64}Cu for use in medical applications. The study focuses on cyclotron based production. The first alternative is a nickel target and the second alternative is a zinc target. Both targets have been evaluated considering target thickness and incident beam angle. The cases for natural and enriched material were also investigated to see the difference in yield. For the nickel target case we have seen that the enriched material gives more than enough activity for PET applications. Although the natural nickel target gives reasonably sufficient yields, it may be hazardous to patient health due to the amount of copper required to achieve the desired specific activity in the final product. The 13 - 25 MeV energy range gives the highest yield for the enriched nickel target. Similar assessments were made for the zinc target in order to evaluate the yields. Unlike the nickel target, the difference between the natural and enriched target is not too great for the zinc target. 30 MeV gives the highest yield for all zinc target configurations.

Although the physical yields and activities appear suitable for medical production, there will be possible losses due to irradiation, target transfer, post-irradiation processes, etc. Overall, losses of 15-20 % can be expected in the final product. Even then, the activities would be sufficient to produce the radiopharmaceutical. This work may lead to ^{64}Cu production at accelerator facilities and help to plan production with great precision.

5. Appendix: Tables

Table 1: Physical yields and activities for the 100 μm thick Nickel target. The table shows the results of both 5° and 10° target angle. The table is divided into two parts: Results of elemental nickel and results of enriched nickel. Energy range is between 10 to 30 MeV. The activity values are given for $I = 200\mu A$ and $t = 3h$.

	Elemental Ni				Enriched ^{64}Ni			
	5°		10°		5°		10°	
Energy (MeV)	P. Y. ($MBq/\mu Ah$)	A. (MBq)	P. Y. ($MBq/\mu Ah$)	A. (MBq)	P. Y. ($MBq/\mu Ah$)	A. (MBq)	P. Y. ($MBq/\mu Ah$)	A. (MBq)
10	2.45	1.47×10^3	2.93	1.76×10^3	3.57×10^2	2.14×10^5	3.46×10^2	2.07×10^5
11	5.04	3.03×10^3	4.29	2.58×10^3	5.01×10^2	3.00×10^5	4.94×10^2	2.96×10^5
12	6.40	3.84×10^3	6.75	4.05×10^3	6.39×10^2	3.83×10^5	6.26×10^2	3.76×10^5
13	5.66	3.39×10^3	5.25	3.15×10^3	7.12×10^2	4.27×10^5	7.16×10^2	4.29×10^5
14	7.90	4.74×10^3	6.34	3.80×10^3	7.79×10^2	4.68×10^5	7.82×10^2	4.69×10^5
15	8.38	5.03×10^3	6.95	4.17×10^3	8.07×10^2	4.84×10^5	8.08×10^2	4.85×10^5
16	8.58	5.15×10^3	7.49	4.50×10^3	8.32×10^2	4.99×10^5	8.21×10^2	4.92×10^5
17	7.84	4.70×10^3	8.04	4.82×10^3	8.45×10^2	5.07×10^5	8.24×10^2	4.95×10^5
18	7.22	4.33×10^3	7.49	4.50×10^3	8.59×10^2	5.15×10^5	7.57×10^2	4.54×10^5
19	7.77	4.66×10^3	6.40	3.84×10^3	8.67×10^2	5.20×10^5	6.63×10^2	3.98×10^5
20	7.63	4.58×10^3	5.72	3.43×10^3	8.47×10^2	5.08×10^5	5.43×10^2	3.26×10^5
21	7.63	4.58×10^3	5.45	3.27×10^3	8.21×10^2	4.93×10^5	4.42×10^2	2.65×10^5
22	6.00	3.60×10^3	3.72	1.96×10^3	7.69×10^2	4.62×10^5	3.37×10^2	2.02×10^5
23	8.79	5.27×10^3	2.93	1.96×10^3	7.03×10^2	4.22×10^5	2.54×10^2	1.52×10^5
24	6.61	3.97×10^3	3.61	2.17×10^3	6.49×10^2	3.89×10^5	2.00×10^2	1.20×10^5
25	5.79	3.47×10^3	2.18	1.31×10^3	5.77×10^2	3.46×10^5	1.76×10^2	1.06×10^5
26	6.68	4.01×10^3	1.77	1.06×10^3	5.08×10^2	3.05×10^5	1.54×10^2	9.24×10^4
27	4.43	2.66×10^3	1.91	1.14×10^3	4.49×10^2	2.69×10^5	1.43×10^2	8.57×10^4
28	3.88	2.33×10^3	1.23	7.36×10^2	4.27×10^2	2.56×10^5	1.23×10^2	7.40×10^4
29	3.41	2.04×10^3	0.954	7.52×10^2	3.71×10^2	2.22×10^5	1.25×10^2	7.51×10^4
30	3.47	2.08×10^3	1.02	6.13×10^2	3.49×10^2	2.09×10^5	1.18×10^2	7.09×10^4

Table 2: Physical yields and activities for the 150 μm thick Nickel target.

	Elemental Ni				Enriched ^{64}Ni			
	5°		10°		5°		10°	
Energy (MeV)	P. Y. ($MBq/\mu Ah$)	A. (MBq)	P. Y. ($MBq/\mu Ah$)	A. (MBq)	P. Y. ($MBq/\mu Ah$)	A. (MBq)	P. Y. ($MBq/\mu Ah$)	A. (MBq)
10	3.68	2.21×10^{3}	3.75	2.52×10^{3}	3.36×10^{2}	2.02×10^{5}	3.56×10^{2}	2.13×10^{5}
11	4.09	2.45×10^{3}	4.29	2.58×10^{3}	4.83×10^{2}	2.90×10^{5}	5.09×10^{2}	3.05×10^{5}
12	4.77	2.86×10^{3}	5.04	3.03×10^{3}	5.97×10^{2}	3.58×10^{5}	6.33×10^{2}	3.80×10^{5}
13	5.38	3.23×10^{3}	5.93	3.56×10^{3}	6.89×10^{2}	4.13×10^{5}	7.27×10^{2}	4.36×10^{5}
14	6.68	4.01×10^{3}	7.09	4.25×10^{3}	7.39×10^{2}	4.43×10^{5}	7.83×10^{2}	4.70×10^{5}
15	7.43	4.46×10^{3}	7.84	4.70×10^{3}	7.72×10^{2}	4.63×10^{5}	8.19×10^{2}	4.92×10^{5}
16	7.90	4.74×10^{3}	8.18	4.91×10^{3}	7.95×10^{2}	4.77×10^{5}	8.43×10^{2}	5.06×10^{5}
17	8.11	4.86×10^{3}	8.52	5.11×10^{3}	7.98×10^{2}	4.79×10^{5}	8.48×10^{2}	5.09×10^{5}
18	7.49	4.50×10^{3}	7.70	4.62×10^{3}	8.24×10^{2}	4.94×10^{5}	8.75×10^{2}	5.25×10^{5}
19	8.31	4.99×10^{3}	8.93	5.36×10^{3}	8.37×10^{2}	5.02×10^{5}	8.82×10^{2}	5.29×10^{5}
20	8.18	4.91×10^{3}	8.72	5.23×10^{3}	8.45×10^{2}	5.07×10^{5}	8.71×10^{2}	5.22×10^{5}
21	8.45	5.07×10^{3}	8.58	5.15×10^{3}	8.70×10^{2}	5.22×10^{5}	8.50×10^{2}	5.10×10^{5}
22	8.99	5.40×10^{3}	8.31	4.99×10^{3}	8.72×10^{2}	5.23×10^{5}	7.68×10^{2}	4.61×10^{5}
23	9.47	5.68×10^{3}	8.58	5.15×10^{3}	8.53×10^{2}	5.12×10^{5}	6.60×10^{2}	3.96×10^{5}
24	7.49	4.50×10^{3}	5.66	3.39×10^{3}	8.77×10^{2}	5.26×10^{5}	5.72×10^{2}	3.43×10^{5}
25	8.18	4.91×10^{3}	4.36	2.62×10^{3}	8.60×10^{2}	5.16×10^{5}	4.74×10^{2}	2.84×10^{5}
26	8.58	5.15×10^{3}	5.31	3.19×10^{3}	8.33×10^{2}	5.00×10^{5}	3.87×10^{2}	2.32×10^{5}
27	7.09	4.25×10^{3}	3.17	1.90×10^{3}	8.01×10^{2}	4.81×10^{5}	3.17×10^{2}	1.90×10^{5}
28	7.15	4.29×10^{3}	3.47	2.08×10^{3}	7.90×10^{2}	4.74×10^{5}	2.72×10^{2}	1.63×10^{5}
29	7.22	4.33×10^{3}	3.47	2.08×10^{3}	7.59×10^{2}	4.55×10^{5}	2.47×10^{2}	1.48×10^{5}
30	7.56	4.54×10^{3}	2.38	1.43×10^{3}	7.24×10^{2}	4.35×10^{5}	2.23×10^{2}	1.34×10^{5}

Table 3: Physical yields and activities for the 100 μm thick Zinc target.

	Elemental Zn				Enriched ^{68}Zn			
	5°		10°		5°		10°	
Energy (MeV)	P. Y. ($MBq/\mu Ah$)	A. (MBq)	P. Y. ($MBq/\mu Ah$)	A. (MBq)	P. Y. ($MBq/\mu Ah$)	A. (MBq)	P. Y. ($MBq/\mu Ah$)	A. (MBq)
10	0.0	0.0	0.0	0.0	0.0	0.0	0.0	0.0
11	0.0	0.0	0.0	0.0	0.0	0.0	0.0	0.0
12	0.0	0.0	0.0	0.0	0.0	0.0	0.0	0.0
13	0.0	0.0	0.0	0.0	0.0	0.0	0.0	0.0
14	6.81×10^{-2}	4.09×10^{1}	0.0	0.0	0.0	0.0	0.0	0.0
15	1.36×10^{-1}	8.18×10^{1}	6.81×10^{-2}	4.09×10^{1}	0.0	0.0	0.0	0.0
16	2.04×10^{-1}	1.23×10^{2}	0.0	0.0	0.0	0.0	0.0	0.0
17	1.36×10^{-1}	$8{,}18 \times 10^{1}$	0.0	0.0	0.0	0.0	0.0	0.0
18	6.81×10^{-2}	4.09×10^{1}	6.81×10^{-2}	4.09×10^{1}	0.0	0.0	0.0	0.0
19	0.0	0.0	1.36×10^{-1}	8.18×10^{1}	6.81×10^{-2}	4.09×10^{1}	0.0	0.0
20	6.81×10^{-2}	4.09×10^{1}	6.81×10^{-2}	4.09×10^{1}	0.0	0.0	0.0	0.0
21	2.73×10^{-1}	1.64×10^{2}	1.36×10^{-1}	8.18×10^{1}	6.81×10^{-1}	4.09×10^{2}	6.81×10^{-1}	4.09×10^{2}
22	4.09×10^{-1}	2.45×10^{2}	6.13×10^{-1}	3.68×10^{2}	2.52×10^{0}	1.51×10^{3}	3.10×10^{0}	1.86×10^{3}
23	1.29×10^{0}	7.7×10^{2}	1.29×10^{0}	7.77×10^{2}	5.59×10^{0}	3.35×10^{3}	6.47×10^{0}	3.88×10^{3}
24	1.70×10^{0}	1.02×10^{3}	2.04×10^{0}	1.23×10^{3}	1.03×10^{1}	5.26×10^{5}	1.06×10^{1}	6.34×10^{3}
25	3.24×10^{0}	1.94×10^{3}	3.27×10^{0}	1.96×10^{3}	1.45×10^{1}	8.69×10^{3}	1.55×10^{1}	9.30×10^{3}
26	3.99×10^{0}	2.39×10^{3}	4.50×10^{0}	2.70×10^{3}	2.07×10^{1}	1.24×10^{4}	2.18×10^{1}	1.31×10^{4}
27	5.35×10^{0}	3.21×10^{3}	4.63×10^{0}	2.78×10^{3}	2.47×10^{1}	1.48×10^{4}	2.76×10^{1}	1.66×10^{4}
28	6.61×10^{0}	3.97×10^{3}	6.95×10^{0}	4.17×10^{3}	3.63×10^{1}	2.18×10^{4}	3.10×10^{1}	1.86×10^{4}
29	9.33×10^{0}	5.60×10^{3}	5.86×10^{0}	3.52×10^{3}	4.32×10^{1}	2.59×10^{4}	3.43×10^{1}	2.06×10^{4}
30	1.15×10^{1}	6.91×10^{3}	6.61×10^{0}	3.97×10^{3}	4.93×10^{1}	2.96×10^{4}	3.58×10^{1}	2.15×10^{4}

Table 4: Physical yields and activities for the 150 μm thick Zinc target.

	Elemental Zn				Enriched ^{68}Zn			
	5°		10°		5°		10°	
Energy (MeV)	P. Y. ($MBq/\mu Ah$)	A. (MBq)	P. Y. ($MBq/\mu Ah$)	A. (MBq)	P. Y. ($MBq/\mu Ah$)	A. (MBq)	P. Y. ($MBq/\mu Ah$)	A. (MBq)
10	0.0	0.0	0.0	0.0	0.0	0.0	0.0	0.0
11	0.0	0.0	0.0	0.0	0.0	0.0	0.0	0.0
12	0.0	0.0	0.0	0.0	0.0	0.0	0.0	0.0
13	0.0	0.0	6.81×10^{-2}	4.09×10^{1}	0.0	0.0	0.0	0.0
14	2.04×10^{-1}	1.23×10^{2}	1.36×10^{-1}	8.18×10^{1}	0.0	0.0	0.0	0.0
15	6.81×10^{-2}	4.09×10^{1}	1.36×10^{-1}	8.18×10^{1}	0.0	0.0	0.0	0.0
16	6.81×10^{-2}	4.09×10^{1}	1.36×10^{-1}	8.18×10^{1}	0.0	0.0	0.0	0.0
17	1.36×10^{-1}	8.18×10^{1}	1.36×10^{-1}	8.18×10^{1}	0.0	0.0	0.0	0.0
18	0.0	0.0	0.0	0.0	0.0	0.0	0.0	0.0
19	2.04×10^{-1}	1.23×10^{2}	1.36×10^{-1}	8.18×10^{1}	0.0	0.0	0.0	0.0
20	0.0	0.0	6.81×10^{-2}	4.09×10^{1}	6.81×10^{-2}	4.09×10^{1}	6.81×10^{-2}	4.09×10^{1}
21	1.36×10^{-1}	8.18×10^{1}	1.36×10^{-1}	8.18×10^{1}	4.09×10^{-1}	2.45×10^{2}	4.09×10^{-1}	2.45×10^{2}
22	6.81×10^{-1}	4.09×10^{2}	6.13×10^{-1}	3.68×10^{2}	2.42×10^{0}	1.45×10^{3}	2.49×10^{0}	1.49×10^{3}
23	1.33×10^{0}	7.97×10^{2}	1.33×10^{0}	7.97×10^{2}	6.03×10^{0}	3.62×10^{3}	6.23×10^{0}	3.74×10^{3}
24	2.45×10^{0}	1.47×10^{3}	2.62×10^{0}	1.57×10^{3}	1.05×10^{1}	6.28×10^{3}	1.10×10^{1}	6.58×10^{3}
25	3.20×10^{0}	1.92×10^{3}	3.42×10^{0}	1.94×10^{3}	1.53×10^{1}	9.18×10^{3}	1.64×10^{1}	9.85×10^{3}
26	3.51×10^{0}	2.11×10^{3}	3.71×10^{0}	2.23×10^{3}	2.0×10^{1}	1.20×10^{4}	2.08×10^{1}	1.25×10^{4}
27	5.42×10^{0}	3.25×10^{3}	5.48×10^{0}	3.29×10^{3}	2.57×10^{1}	1.54×10^{4}	2.70×10^{1}	1.62×10^{4}
28	7.56×10^{0}	4.54×10^{3}	7.77×10^{0}	4.66×10^{3}	3.50×10^{1}	2.10×10^{4}	3.69×10^{1}	2.21×10^{4}
29	8.99×10^{0}	5.40×10^{3}	9.47×10^{0}	5.68×10^{3}	3.95×10^{1}	2.37×10^{4}	4.02×10^{1}	2.41×10^{4}
30	9.54×10^{0}	5.72×10^{3}	9.44×10^{0}	5.66×10^{3}	4.96×10^{1}	2.97×10^{4}	4.81×10^{1}	2.89×10^{4}

References

[1] S. Baruta, R. Leonte, D. Cocioaba, L. Craciun, C. A. Ur, D. Niculae, Cyclotron production of 64cu by proton irradiation of enriched 64ni target: Validation of geant4 simulation parameters through experimental data, Frontiers in Physics 10 (2022) 1240. doi:10.3389/fphy.2022.1038014.

[2] R. Chakravarty, A. Rajeswari, P. Shetty, K. Jagadeesan, R. Ram, S. Jadhav, H. D. Sarma, A. Dash, S. Chakraborty, A simple and robust method for radiochemical separation of no-carrier-added 64cu produced in a research reactor for radiopharmaceutical preparation, Applied Radiation and Isotopes 165 (2020) 109341. doi:10.1016/j.apradiso.2020.109341.

[3] G. Dellepiane, P. Casolaro, I. Mateu, P. Scampoli, N. Voeten, S. Braccini, Cross-section measurement for an optimized 61cu production at an 18 mev medical cyclotron from natural zn and enriched 64zn solid targets, Applied radiation and isotopes 190 (2022) 110466. doi:10.1016/j.apradiso.2022.110466.

[4] G. Dellepiane, P. Casolaro, I. Mateu, P. Scampoli, S. Braccini, Alternative routes for 64cu production using an 18 mev medical cyclotron in view of theranostic applications, Applied radiation and isotopes 191 (2023) 110518. doi:10.1016/j.apradiso.2022.110518.

[5] I. Kambali, I. R. Febrianto, R. Ritawidya, R. D. Haryuni, On the study of cu-64 production from 18 mev proton-induced secondary fast neutron bombardment, Journal of the Korean Physical Society (2022) 1–6doi:10.1007/s40042-022-00697-3.

[6] M. Kawabata, S. Motoishi, A. Ohta, A. Motomura, H. Saeki, K. Tsukada, S. Hashimoto, N. Iwamoto, Y. Nagai, K. Hashimoto, Large scale production of 64 cu and 67 cu via the 64 zn (n, p) 64 cu and 68 zn (n, np/d) 67 cu reactions using accelerator neutrons, Journal of Radioanalytical and Nuclear Chemistry 330 (2021) 913–922. doi:10.1007/s10967-021-07987-3.

[7] T. Wadas, E. Wong, G. Weisman, C. Anderson, Copper chelation chemistry and its role in copper radiopharmaceuticals, Current pharmaceutical design 13 (1) (2007) 3–16. doi:10.2174/138161207779313768.

[8] J. Svedjehed, C. J. Kutyreff, J. W. Engle, K. Gagnon, Automated, cassette-based isolation and formulation of high-purity [61cu] cucl2 from solid ni targets, EJNMMI Radiopharmacy and Chemistry 5 (1) (2020) 1–14. doi:10.1186/s41181-020-00108-7.

[9] IAEA., Alternative Radionuclide Production with a Cyclotron, International Atomic Energy Agency, 2021.

[10] K. Abbas, J. Kozempel, M. Bonardi, F. Groppi, A. Alfarano, U. Holzwarth, F. Simonelli, H. Hofman, W. Horstmann, E. Menapace, et al., Cyclotron production of 64cu by deuteron irradiation of 64zn, Applied radiation and isotopes 64 (9) (2006) 1001–1005. doi:10.1016/j.apradiso.2005.12.021.

[11] M. Capogni, M. Capone, A. Pietropaolo, A. Fazio, G. Dellepiane, R. Falconi, A. Colangeli, S. Palomba, G. Valentini, M. Fantuzi, et al., 64cu production by 14 mev neutron beam, Journal of Neutron Research 22 (2-3) (2020) 257–264. doi:10.3233/JNR-190140.

[12] F. Szelecsényi, G. Steyn, Z. Kovács, C. Vermeulen, N. Van Der Meulen, S. Dolley, T. Van Der Walt, K. Suzuki, K. Mukai, Investigation of the 66zn (p, 2pn) 64cu and 68zn (p, x) 64cu nuclear processes up to 100 mev: Production of 64cu, Nuclear Instruments and Methods in Physics Research Section B: Beam Interactions with Materials and Atoms 240 (3) (2005) 625–637. doi:10.1016/j.nimb.2005.05.057.

[13] F. Szelecsényi, Z. Kovács, K. Nagatsu, M.-R. Zhang, K. Suzuki, Excitation function of (p, α) nuclear reaction on enriched 67zn: possibility of production of 64cu at low energy cyclotron, Radiochimica Acta 102 (6) (2014) 465–472. doi:10.1515/ract-2013-2145.

[14] J. Ometáková, P. Rajec, V. Csiba, M. Leporis, M. Štefečka, P. Vlk, M. Galamboš, O. Rosskopfova, Automated production of 64 cu prepared by 18 mev cyclotron, Journal of Radioanalytical and Nuclear Chemistry 293 (1) (2012) 217–222. doi:10.1007/s10967-012-1757-3.

[15] D. W. McCarthy, R. E. Shefer, R. E. Klinkowstein, L. A. Bass, W. H. Margeneau, C. S. Cutler, C. J. Anderson, M. J. Welch, Efficient production of high specific activity 64cu using a biomedical cyclotron, Nuclear medicine and biology 24 (1) (1997) 35–43. doi:10.1016/S0969-8051(96)00157-6.

[16] J. C. Manrique-Arias, M. A. Avila-Rodriguez, A simple and efficient method of nickel electrodeposition for the cyclotron production of 64cu, Applied Radiation and Isotopes 89 (2014) 37–41. doi:10.1016/j.apradiso.2014.01.024.

[17] H. A. Williams, S. Robinson, P. Julyan, J. Zweit, D. Hastings, A comparison of pet imaging characteristics of various copper radioisotopes, European journal of nuclear medicine and molecular imaging 32 (2005) 1473–1480. doi:10.1007/s00259-005-1906-9.

[18] J. Y. Kim, H. Park, J. C. Lee, K. M. Kim, K. C. Lee, H. J. Ha, T. H. Choi, G. I. An, G. J. Cheon, A simple cu-64 production and its application of cu-64 atsm, Applied Radiation and Isotopes 67 (7-8) (2009) 1190–1194. doi:10.1016/j.apradiso.2009.02.060.

[19] I. Novak-Hofer, A. P. Schubiger, Copper-67 as a therapeutic nuclide for radioimmunotherapy, European journal of nuclear medicine and molecular imaging 29 (2002) 821–830. doi:10.1007/s00259-001-0724-y.

[20] J. Howse, M. Zaw, P. Pellegrini, A. Katsifis, I. Greguric, R. Weiner, et al., Alternative method for 64cu radioisotope production, Applied Radiation and Isotopes 67 (7-8) (2009) 1324–1331. doi:10.1016/j.apradiso.2009.02.069.

[21] P. J. Blower, J. S. Lewis, J. Zweit, Copper radionuclides and radiopharmaceuticals in nuclear medicine, Nuclear Medicine and Biology 23 (8) (1996) 957–980. doi:https://doi.org/10.1016/S0969-8051(96)00130-8.

[22] C. J. Anderson, R. Ferdani, Copper-64 radiopharmaceuticals for pet imaging of cancer: advances in preclinical and clinical research, Cancer Biotherapy and Radiopharmaceuticals 24 (4) (2009) 379–393. doi:10.1089/cbr.2009.0674.

[23] V. Bechtold, Isotope production with cyclotronsdoi:10.5170/CERN-1996-002.329.

[24] H. Thisgaard, M. Jensen, D. R. Elema, Medium to large scale radioisotope production for targeted radiotherapy using a small pet cyclotron, Applied Radiation and Isotopes 69 (1) (2011) 1–7. doi:10.1016/j.apradiso.2010.07.019.

[25] W. Z. Gelbart, R. R. Johnson, Solid target system with in-situ target dissolution, Instruments 3 (1) (2019) 14. doi:10.3390/instruments3010014.

[26] S. Agostinelli, J. Allison, K. a. Amako, J. Apostolakis, H. Araujo, P. Arce, M. Asai, D. Axen, S. Banerjee, G. Barrand, et al., Geant4—a simulation toolkit, Nuclear instruments and methods in physics research section A: Accelerators, Spectrometers, Detectors and Associated Equipment 506 (3) (2003) 250–303. doi:10.1016/S0168-9002(03)01368-8.

[27] J. Allison, K. Amako, J. Apostolakis, H. Araujo, P. A. Dubois, M. Asai, G. Barrand, R. Capra, S. Chauvie, R. Chytracek, et al., Geant4 developments and applications, IEEE Transactions on nuclear science 53 (1) (2006) 270–278. doi:10.1109/TNS.2006.869826.

[28] J. Allison, K. Amako, J. Apostolakis, P. Arce, M. Asai, T. Aso, E. Bagli, A. Bagulya, S. Banerjee, G. Barrand, et al., Recent developments in geant4, Nuclear instruments and methods in physics research section A: Accelerators, Spectrometers, Detectors and Associated Equipment 835 (2016) 186–225. doi:10.1016/j.nima.2016.06.125.

[29] F. Poignant, S. Penfold, J. Asp, P. Takhar, P. Jackson, Geant4 simulation of cyclotron radioisotope production in a solid target, Physica Medica 32 (5) (2016) 728–734. doi:10.1016/j.ejmp.2016.04.006.

[30] R. Brun, F. Rademakers, Root — an object oriented data analysis framework, Nuclear Instruments and Methods in Physics Research Section A: Accelerators, Spectrometers, Detectors and Associated Equipment 389 (1) (1997) 81–86, new Computing Techniques in Physics Research V. doi:10.1016/S0168-9002(97)00048-X.

[31] F. Szelecsényi, G. Blessing, S. Qaim, Excitation functions of proton induced nuclear reactions on enriched 61ni and 64ni: Possibility of production of no-carrier-added 61cu and 64cu at a small cyclotron, Applied Radiation and Isotopes 44 (3) (1993) 575–580. doi:10.1016/0969-8043(93)90172-7.

[32] M. A. Avila-Rodriguez, J. A. Nye, R. J. Nickles, Simultaneous production of high specific activity 64cu and 61co with 11.4 mev protons on enriched 64ni nuclei, Applied Radiation and Isotopes 65 (10) (2007) 1115–1120. doi:10.1016/j.apradiso.2007.05.012.

[33] M. Aslam, S. Sudár, M. Hussain, A. Malik, H. Shah, S. M. Qaim, Charged particle induced reaction cross section data for production of the emerging medically important positron emitter 64cu: a comprehensive evaluation, Radiochimica Acta 97 (12) (2009) 669–686. doi:10.1524/ract.2009.1670.

[34] R. A. Rebeles, P. Van den Winkel, A. Hermanne, F. Tárkányi, New measurement and evaluation of the excitation function of 64ni (p, n) reaction for the production of 64cu, Nuclear Instruments and Methods in Physics Research Section B: Beam Interactions with Materials and Atoms 267 (3) (2009) 457–461. doi:10.1016/j.nimb.2008.11.038.